Vision Research 107 (2015) 86–93

Contents lists available at ScienceDirect

Vision Research

journal homepage: www.elsevier.com/locate/visres

3D surface configuration modulates 2D symmetry detection

Chien-Chung Chen [a,b,*], Lok-Teng Sio [a]

[a] Department of Psychology, National Taiwan University, Taipei, Taiwan
[b] Neurobiology and Cognitive Science Center, National Taiwan University, Taipei, Taiwan

ARTICLE INFO

Article history:
Received 10 June 2014
Received in revised form 8 December 2014
Available online 20 December 2014

Keywords:
Coplanarity
Depth
Three-dimensional
Slant
Shape

ABSTRACT

We investigated whether three-dimensional (3D) information in a scene can affect symmetry detection. The stimuli were random dot patterns with 15% dot density. We measured the coherence threshold, or the proportion of dots that were the mirror reflection of the other dots in the other half of the image about a central vertical axis, at 75% accuracy with a 2AFC paradigm under various 3D configurations produced by the disparity between the left and right eye images. The results showed that symmetry detection was difficult when the corresponding dots across the symmetry axis were on different frontoparallel or inclined planes. However, this effect was not due to a difference in distance, as the observers could detect symmetry on a slanted surface, where the depth of the two sides of the symmetric axis was different. The threshold was reduced for a hinge configuration where the join of two slanted surfaces coincided with the axis of symmetry. Our result suggests that the detection of two-dimensional (2D) symmetry patterns is subject to the 3D configuration of the scene; and that coplanarity across the symmetry axis and consistency between the 2D pattern and 3D structure are important factors for symmetry detection.

Symmetry occurs when one part of an image is the reflection of the other part about an axis. It is often one of the most salient features in a scene (Koffka, 1935) and can easily be detected by a human observer (Barlow & Reeves, 1979; Carmody, Nodine, & Locher, 1977; Corballis & Roldan, 1975; Tyler, Hardage, & Miller, 1995; Wagemans, 1995).

Symmetry is important in order for an observer to perceive a three-dimensional (3D) object. A two-dimensional (2D) image, such as a retinal image, can be a projection of an infinite number of possible 3D objects. Hence, computationally, it is impossible to solve this many-to-one mapping problem and recover the 3D shape of an object from only one 2D image. However, by assuming that the object is symmetric, one can constrain the computation enough to recover the 3D shape of an object from a single 2D image (Kanade, 1981; Li et al., 2011; Pizlo, Sawada, Li, Kropatsch, & Steinman, 2010; Vetter & Poggio, 1994; Pizlo, Li, Sawada & Steinman, 2014). This assumption is reasonable because a large proportion of the objects that we encounter in daily life, especially those relevant to the survival of an animal, such as potential predators, food sources or mates, are symmetric (Carmody et al., 1977; Corballis & Roldan, 1975; Tyler et al., 1995). Thus, it is likely that there are mechanisms in the visual system specialized for symmetric 3D objects (for a review, see Tyler, 1994). In addition, there is evidence showing that a human observer does assume symmetry in 3D shape perception (Li et al., 2011; Pizlo et al., 2010; Sawada & Pizlo, 2008; Wagemans, 1993) and that it is easier for human observers to discriminate between symmetric 3D objects than asymmetric ones (Liu & Kersten, 2003).

Although symmetry is important in the perception of a 3D shape, it is not clear whether the shape of a 3D object can affect the detection of symmetry *per se*. Since a large number of the studies on symmetry perception have had their stimuli presented either on a piece of paper or a computer controlled monitor screen (for a review, see Wagemans, 1995), it should be obvious that a human observer can detect symmetry on a frontoparallel plane with no obvious 3D structure. Indeed, current theories of symmetry perception (e.g., Chen & Tyler, 2010; Dakin & Hess, 1997; Osorio, 1996; Poirier & Wilson, 2010; Rainville & Kingdom, 1999, 2000; Scognamillo, Rhodes, Morrone, & Burr, 2003; Tjan & Liu, 2005; van der Helm & Leeuwenberg, 1996; Wagemans, 1993) focus on the computation of 2D retinal images and do not consider the 3D structure of the scene.

If symmetry perception depends only on an analysis of 2D retinal images, the 3D structure of the scene should have no effect on symmetry detection. Hence, an observer should perceive symmetry equally well in a retinal image projected by a symmetric 3D

* Corresponding author at: Department of Psychology, National Taiwan University, Taipei, Taiwan.
E-mail address: c3chen@ntu.edu.tw (C.-C. Chen).

http://dx.doi.org/10.1016/j.visres.2014.12.007
0042-6989/

objector in a symmetric paint on the surface of an asymmetric object. To test this hypothesis, we manipulated a hinge-like 3D structure of the scene with binocular disparity. The hinge-like structure consisted of two slanted surfaces which met at one edge, while the axis of the symmetric pattern might or might not be coincident with the dihedral edge of the 3D shape. A symmetry perception mechanism that is based on the analysis of 2D images would be indifferent to any correspondence between the 3D dihedral edge and the symmetry axis. On the other hand, if the visual mechanism detects symmetric 3D objects, it would detect symmetry more easily when it is consistent with the 3D structure of the scene. In our study, we expected a lower detection threshold when the 3D dihedral edge coincided with the symmetry axis than in any other conditions.

In addition to 3D shape recovery, symmetry computation in the visual system may interact with 3D vision in another way. To perceive symmetry, the visual system needs to find a correspondence between image elements across a symmetry axis (Csatho, van der Vloed, & van der Helm, 2004; Dakin & Hess, 1997; Dakin & Watt, 1994; Gurnsey, Herbert, & Kenemy, 1998; Poirier & Wilson, 2010; Rainville & Kingdom, 1999, 2000; Scognamillo et al., 2003; Tjan & Liu, 2005; van der Helm & Leeuwenberg, 1996; Wagemans, 1993; Wu & Chen, 2014). Recently, it has been shown that lateral interaction is subject to depth information in the scene (Huang, Hess, & Dakin, 2006; Tyler & Kontsevich, 1995; Huang, Chen, & Tyler, 2012). For instance, it is known that the visibility of a target stimulus can be modulated by the presence of a flanker presented elsewhere in the scene (Chen & Tyler, 2001, 2002, 2008; Polat & Sagi, 1993, 1994). Huang et al. (2006) showed that this lateral effect can be abolished when the target and flanker are presented at different depths. Further investigation found that the lateral effect can occur when the target and flanker are at different depths, as long as they can be perceived as being on the same slant plane (Huang et al., 2012). On the other hand, this lateral effect can be abolished when the target and flanker are presented at the same depth but perceived on different parallel planes, for example, on different saw teeth (Huang et al., 2012). Hence, it seems that it is coplanarity, rather than depth *per se*, which affects lateral interaction. Inspired by this result, we also manipulated the depth of the image elements on different halves of the symmetry axis, allowing us to observe the effect of coplanarity.

1. Method

1.1. Observers

Five college students recruited from National Taiwan University participated in the experiments. All observers were naïve to the purpose of this study. They had normal or corrected-to-normal visual acuity (20/20). The stereopsis of the observers was tested by identifying the direction (concave or convex) of a wedge stimulus (see Section 1.3). All observers passed the test. This study was approved by the Research Ethic Committee of National Taiwan University and the conduct of the experiment followed the guidelines of Helsinki Declaration and local regulations. Written consent was obtained from each observer before the experiment.

1.2. Apparatus

The stimuli were presented on a 19-inch CRT monitor with 1024(H) × 768(V) spatial resolution and an 85 Hz refresh rate, controlled by a MacPro computer. The viewing field was 19.8° (H) by 14.6° (V). The display was divided into two halves with the left-eye image presented on the left side of the display, and the right-eye image on the right side of the display. Observers viewed the stimuli through a 4-mirror stereoscope in a dark, quiet room. The observers' heads were supported by a chin rest. To avoid cross-talk between the left and right images, a black board was placed in front of the display and extended between the two central viewing mirrors of the stereoscope. The viewing distance, through the optical path from the display, passing the two mirrors to the eye, was 110 cm. At this viewing distance one pixel on the screen subtended 0.019 × 0.019°. The monitor input-output intensity function was calibrated with a Photo Research (Chatsworth, CA, USA) PR655 radiometer. The experimental control and the stimulus generation were written in MATLAB with the Psychophysics Toolbox (Brainard, 1997).

1.3. Stimuli

The stimuli were random-dot stereograms composed of black dots on a dark gray background. The density of the random dots was 15%. Each dot was a 0.095 × 0.095° square. The size of the stimulus for each eye was 5.7 × 5.7°. Each image contained a symmetric component, in which each half was mirrored from the other half about a central vertical axis, and a random component, in which the location of the dots was determined by a uniform random number generator. The visibility of the symmetry was measured in coherence, which was the number of dots in the symmetric component divided by the total number of dots in an image.

The dots in the image presented to one of the two eyes (the dominant eye) were displaced according to a depth map to produce a disparity. The disparity was computed with

$$\eta(x,y) = \frac{\alpha\, d(x,y)}{d^2} \tag{1}$$

where x and y were the position of a pixel relative to the center of the display in cm; η was the disparity in radiance, d was the viewing distance and was set at 110 cm; Δd was the depth difference from the horopter in cm as defined by a depth map (discussed below); α was the interpupillary distance of 6.5 cm. The displacement was presented to the non-dominant eye of the observer.

The horopter was established with a random dot rectangular frame (7.1° × 7.1°, 1.4° width) surrounding the test stimulus. The surrounding frame was the same for both eyes. The test stimulus was always at the center and changed in configuration depending on the conditions.

There were eleven 3D configurations used in this study. Table 1 lists their names, mathematical definitions, illustration of depth and examples. These configurations were:

(a) Frontoparallel: The whole stimulus was flat and on the fixation plane. This was our baseline condition.
(b) Step: The stimulus contained a frontoparallel surface to the left of the symmetry axis and another to the right. One surface was in front of the fixation plane, while the other surface was behind it. Thus, the corresponding dots of a symmetry pair would be at different depths and on different surfaces.
(c) Random checkerboard: The image was divided into 100 (10 × 10) squares. Each square was flat and had a depth drawn from a uniform distribution.
(d) Yaw: The surface was rotated about the vertical axis, appearing to be slanted to the left or right. Thus, the corresponding dots of a symmetry pair would be at different depths but on the same surface.
(e) Pitch: The stimulus was on a surface rotated about the horizontal axis, looking like an inclined surface. This 3D configuration was similar to (c), but the corresponding dots of a symmetry pair would be at the same depth.

Table 1
The 3D configurations of the stimuli. The first column is the name of the condition. The second column is the mathematical definition of the condition. If not stated otherwise, $d = 5.7$ cm and $a = 1$. The third column illustrates possible percept experienced by the observers. The fourth column visualizes the depth map in each condition. Here, brighter shade means the stimulus element is closer to the observer, and darker shade, further. The fourth column shows examples of the stimuli, with left eye image on the left and right eye image on the right separated by a gray stripe in the middle.

Condition	Definition	Depth map	Illustration	Example
Frontoparallel	z=0	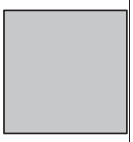		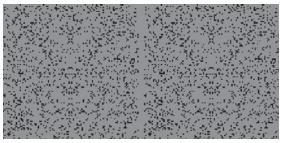
Step	Z = d if x >= 0 Z = -d if x < 0		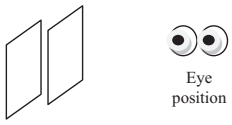	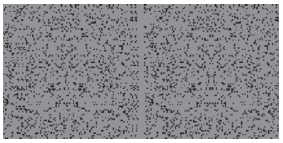
Random checkerboard	Z ~ u(-d, d)	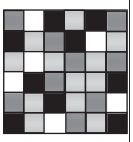	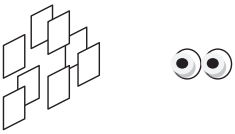	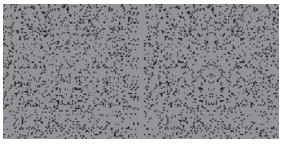
Yaw	Z = a * x		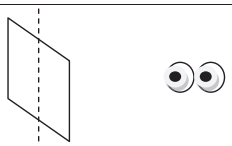	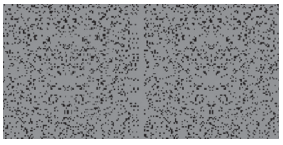
Pitch	Z = a * y		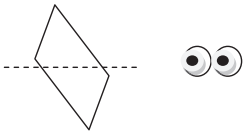	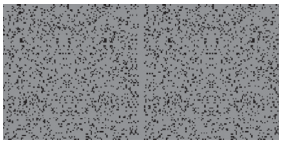
Vertical Shear	Z = a * y if x >= 0 Z = -a * y if x < 0		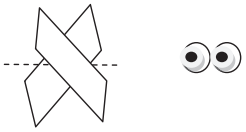	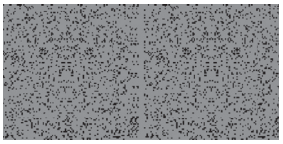
Horizontal shear	Z = a * x if y >= 0 Z = -a * x if y < 0		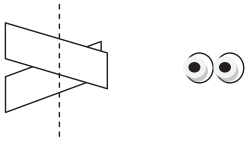	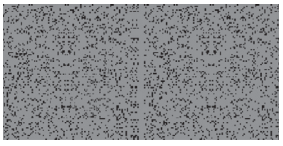
Vertical hinge	Z = a* |x|	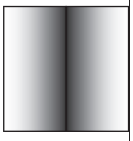	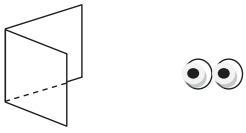	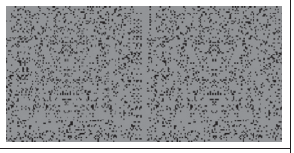
Horizontal hinge	Z = a* |y|		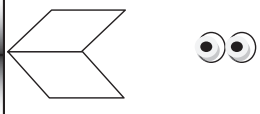	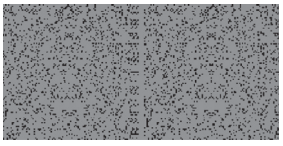
3/4 hinge	Z = a*(|x – 2.5|-2.5)	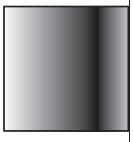	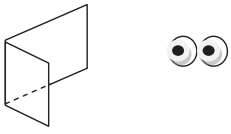	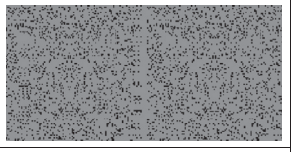
Diagonal hinge	Z = a *(x + y) if x > y Z = a* (x – y) if x < y		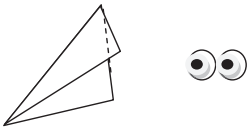	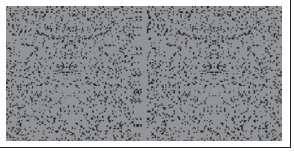

(f) Vertical shear: The surface to the left of the symmetry axis pitched in one direction and the surface to the right pitched in the opposite direction. The corresponding dots of a symmetry pair would be at different depths and on different surfaces.
(g) Horizontal shear: The surface above the fixation yawed in one direction and the one below the fixation yawed in the opposite direction. The corresponding dots of a symmetry pair would be at different depths but on the same surface.
(h) Vertical hinge: This stimulus contained two surfaces slanted in opposite directions, joined at the center of the display. The corresponding dots of a symmetry pair would be at the same depths but on different surfaces. However, the stimulus could be perceived as part of a coherent 3D object.
(i) Horizontal hinge: This was the same as the vertical hinge, but rotated 90°. The corresponding dots of a symmetry pair would be at the same depths and on the same surfaces.
(j) 3/4 hinge: This was similar to a vertical hinge. However, the surfaces joined halfway between the center and either the left or right edge of the stimulus. Thus, the edges of the surfaces did not coincide with the symmetry axis.
(k) Diagonal hinge: This was a vertical hinge rotated 45°.

Unless stated otherwise, the pitch or yaw was 45° in (d–k). The range of depth was +/− 5.7 cm in (b) and (c).

The stimuli can be roughly organized into three groups. The first group, (a–c), were all composed of flat surfaces. These were to test the depth effect. The second, (d–g), had surfaces with linear depth modulation, and were designed to examine the coplanar effect. The third group, (h–k), had a non-monotonic depth modulation across the stimulus, and were designed to examine where the consistency between 3D shape and 2D pattern would have an effect on symmetry detection.

1.4. Procedure

We measured the coherence threshold for symmetry detection with a temporal 2AFC paradigm. In each trial, a fixation cross (+) was first presented to the observers. The upper vertical bar and the horizontal bar were presented to the left eye and the lower vertical bar and the horizontal bar were presented to the right eye. The observers were required to align these two parts to obtain an intact plus sign. After fixation, the first stimulus interval was presented for 500 ms, followed by a blank interval with a duration of 200 ms and the second interval. One interval contained a symmetric target of a certain coherence or a noise distractor (zero coherence). The target appeared randomly in either of the two intervals. The task of the observers was to indicate which interval contained a target. The coherence threshold was measured with a PSI adaptive threshold-seeking algorithm (Kontsevich & Tyler, 1999) at 75% percentage correct level. Each data point reported was the average of at least four measurements.

2. Result

2.1. Coplanar effect

Fig. 1 shows the averaged coherence threshold for symmetry detection in different linear configuration conditions. We used paired *t*-tests to compare the coherence threshold in different 3D conditions to the frontoparallel condition. The coherence threshold in the step condition (49%) was significantly larger than in the frontoparallel condition (43.48%, $t(4) = 6.13$, Bonferroni corrected $p = 0.019 < \alpha = .05$). The Bayesian factor (B_{01}) for this difference, computed with Bayesian information criterion (BIC, Masson, 2011; Rouder, Speckman, Sun, & Iverson, 2009; Wagenmaker, 2007), was .34 (posterior probability $p_{BIC}(H_1|D) = .75$), indicating a substantial effect size for this difference. This result is consistent with that reported in Bertone and Faubert (2002). The coherence threshold for the random checkerboard condition (67.78%) was also much greater than that for the frontoparallel condition ($t(4) = 9.73$, corrected $p = .0034$). The Bayesian factor B_{01} was .06, $p_{BIC}(H_1|D) = .94$, indicating a very large effect size.

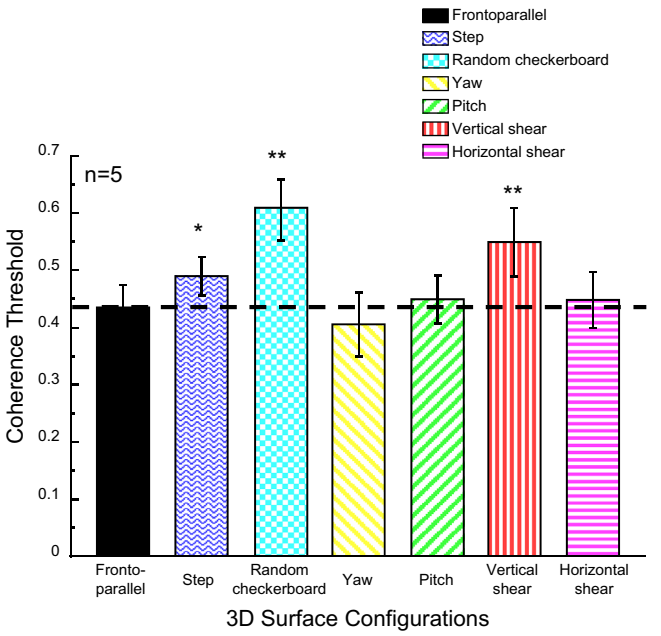

Fig. 1. Coherence threshold in conditions with plane or linear depth modulation, averaged over five observers. For comparison, the dashed line indicates the threshold level for the frontoparallel condition. The "*" and "**" represent significant difference from the frontoparallel threshold at Bonferroni corrected *a*-level .05 and .01, respectively. The error bar represents one standard deviation.

For stimuli with linear depth modulation, the coherence thresholds for the yaw (40.53%) and pitch (44.79%) conditions were not significantly different from those of the frontoparallel condition. The threshold for the vertical shear condition (54.76%) increased dramatically from that for the frontoparallel condition ($t(4) = 8.69$, corrected $p = .0053$; $B_{01} = .16$, $p_{BIC}(H_1|D) = .85$). By contrast, there was no threshold change between the horizontal shear (44.66%) and frontoparallel conditions.

2.2. "Hinges"

Fig. 2 shows the averaged coherence threshold in the hinge conditions. The threshold for the frontoparallel condition is replotted here for comparison. The coherence threshold was significantly reduced for the vertical hinge (30%) as compared to the frontoparallel conditions ($t(4) = 9.08$, corrected $p = .0004$; $B_{01} = .11$, $p_{BIC}(H_1|D) = .99$), while the coherence threshold for the horizontal hinge was not significantly different from that for the frontoparallel condition ($t(4) = 1.7$, corrected $p = 0.6098$; $B_{01} = .73$, $p_{BIC}(H_1|D) = .65$). That is, even though these two hinge conditions had the same depth information, they produced different results. The difference between the vertical and horizontal hinge conditions may be due to whether the join of the two surfaces coincided with the symmetry axis. This hypothesis was further confirmed by a lack of change in coherence threshold from that of the frontoparallel in both the 3/4 hinge (40%) and diagonal hinge (38%). The former was just a vertical hinge shift to the horizontal while the latter was a vertical hinge rotated 45°. Thus these stimuli should have the same depth information as the vertical hinge but lack a correspondence

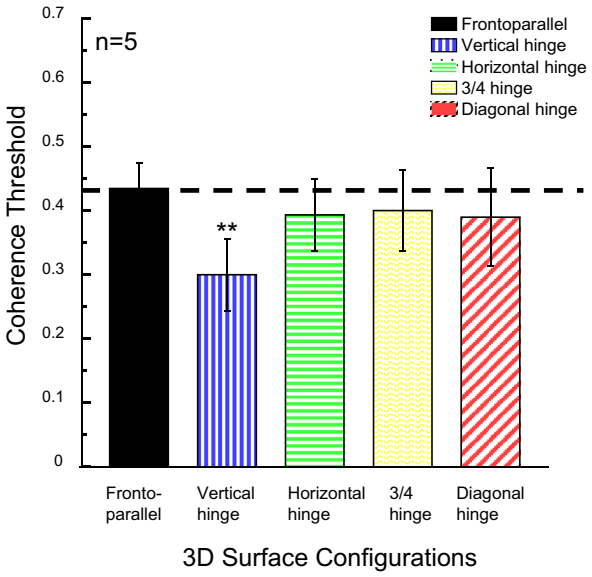

Fig. 2. Coherence threshold in the five hinge conditions, averaged over five observers. The frontoparallel threshold is re-plotted here for comparison. The dashed line indicates the threshold level for the frontoparallel condition. The "**" represents significant difference from the frontoparallel threshold at Bonferroni corrected *a*-level .01. The error bar represents one standard deviation.

between the symmetry axis and the join of the two slanted surfaces. Locher and Smets (1992) also showed that there was no difference in accuracy for detecting a symmetric pattern on a frontoparallel plane and on a plane yawed by 22.5°. van der Vloed, Csathó, and van der Helm (2005), on the other hand, reported that the error rate and reaction time for symmetry detection increased with slant angle. However, in their experiment, the stimuli were orthographic projections of slanted surfaces. Thus, the width of the stimulus decreased with slant angle, and the deterioration of performance in their result may result from the decrease in stimulus size rather than the increase of slant angle.

2.3. Slant angle effect

We further investigated how the magnitude of the 3D modulation affects symmetry detection. The data reported above were acquired with surfaces rotated (either yaw or pitch) 45° from the frontoparallel plane. Here, we measured the symmetry coherence threshold in four 3D conditions (vertical hinge, vertical shear, yaw and pitch) at slant angles from 0° (frontoparallel) to 75°. Fig. 3 shows the result. The gray area in Fig. 3 denotes 99% confidence interval for the frontoparallel threshold.

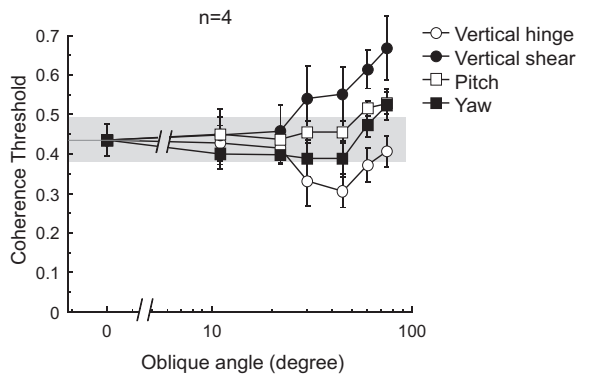

Fig. 3. The effect of rotation (yaw or pitch) angle averaged over four observers in four conditions (vertical hinge, vertical shear, pitch, and yaw). The error bar is one standard deviation of the mean. The gray shaded area is 99% confidence interval.

In the vertical shear condition (solid circles), the coherence threshold increased monotonically with slant angle. The threshold beyond 30° slant angle was significantly different from that in the frontoparallel condition. In the vertical hinge condition (open circles), the threshold first decreased with slant angle, then increased back to the frontoparallel level, with peak facilitation occurring near 45°. The yaw (solid squares) and pitch (open squares) had almost no influence on symmetry detection, though there were signs that the threshold might increase at a high slant angle.

3. Discussion

In this study, we measured the coherence threshold for symmetry detection in 2D patterns rendered on the surfaces of various 3D structures. Compared to the frontoparallel plane, the observers had more difficulty detecting symmetry in the step (Configuration b), random (Configuration c) and vertical shear (Configuration f) conditions, but found it much easier to detect symmetry in the vertical hinge (Configuration h) condition. The symmetry detection in the yaw (Configuration d), pitch (Configuration e), horizontal shear (Configuration g), and non-vertical hinge conditions (Configuration i–k) was similar to that in the frontoparallel conditions.

The threshold increment in the step condition was consistent with that reported by Bertone and Faubert (2002), who also showed that symmetry detection was difficult in a 3D configuration similar to ours. Some other visual phenomena which require a lateral interaction between image components also show similar depth effects. For instance, while the detection of a Gabor pattern can be facilitated by the presence of collinear iso-oriented Gabor flankers (Chen & Tyler, 2001, 2008; Polat & Sagi, 1993), this facilitation effect can be abolished if the target and the flanker are placed on different frontoparallel planes and at different depths (Huang, Chen, & Tyler, 2012; Huang et al., 2006). The tilt illusion induced by an oriented surround can also be reduced if the target and the surround are at different depths (Qiu, Kersten, & Olman, 2013).

As in the step condition, the observers also had a more difficult time detecting symmetry in the random checkerboard condition than in the frontoparallel condition. In the random checkerboard condition, the stimulus was composed of 10 × 10 pieces, each with its own depth. Hence, chances were that the corresponding dots across the symmetry axis would be at different depths. Thus, at first glance, it seems that to detect symmetry, it is necessary for the corresponding dots across the symmetry axis to have the same depth.

However, as it turns out, depth difference is not the critical factor. In our experiment, in the yaw condition, the corresponding dots across the symmetry axis were at different depths. Thus, to detect symmetry, an observer would need to compare the corresponding dots across depths. Similarly, in the pitch condition, the observer needed to compare candidate dot pairs at different depths to determine whether those pairs had the same symmetry axis. Yet, our observers could detect symmetry on yaw and pitch as well as they did on the frontoparallel plane. The major difference was that in both the step and random checkerboard conditions, corresponding dots in the symmetry patterns were not only at different depths but also on different surfaces, while in the yaw and pitch conditions, all dots were on the same slanted surface despite the difference in depth. Hence, symmetry detection would not be affected by depth difference in the scene, as long as all the stimuli were coplanar. There are other visual phenomena that require a lateral interaction between image components which show a

similar coplanar effect. For instance, in the flanker effect discussed above, facilitation from the flanker can be observed when the target and flanker are coplanar, regardless of their depth difference (Huang et al., 2012). The detectability of a contour consisting of dots embedded in noise on a slanted surface was invariant with the yaw angle (Utall, 1983). Recognition of the shape of a pair of figures, symmetric or not, was not affected by the yaw of the presentation plane in the test phase (De Kuijer, Deregowski, & McGeorge, 2004). Thus, it is likely coplanarity, not depth, that is important for perceiving patterns and objects.

With this coplanarity effect in mind, symmetry detection in the two shear conditions can easily be understood. The vertical shear in our experiment was a combination of two surfaces pitched in opposite directions while the horizontal shear was a 90° rotation of the vertical shear. Hence, the amount of 3D information in these two conditions should be the same. Yet, we observed that the observer had a more difficult time detecting symmetry in the vertical shear condition than in the horizontal shear condition. A possible explanation is that since the two sides of the symmetry axis are in different surfaces in the vertical shear condition, the corresponding dots in a symmetry pair are not coplanar. Without coplanarity, the symmetry percept deteriorates. On the other hand, in the horizontal shear condition, while the corresponding dots of a symmetry pair are at different depths, each pair can be taken as being on the same surface. Thus, coplanarity is satisfied for each dot pair. It is true that, in the horizontal shear condition, the upper and lower parts of the stimulus are not coplanar. However, our result implies that either pairwise or local (i.e., only half of the image) coplanarity may be sufficient to support symmetry detection.

Symmetry detection was better in the vertical hinge condition than in the frontoparallel condition. The 3D configuration for the vertical hinge was two slanted surfaces, yawed in the same angle but in opposite directions, joined at the center of the display. The depth modulation was symmetric around the central vertical axis. The vertical hinge could be viewed as a representation of a symmetric object whose symmetry axis was coincident with the symmetry axis of the 2D pattern. Thus, it is easier to detect a 2D symmetry pattern if it is projected on a 3D symmetric object. However, this facilitation effect occurs only if the two symmetry axes match each other. We did not find a facilitation effect in the 3/4 hinge, which was a laterally shifted copy of the vertical hinge, nor in the horizontal or diagonal hinges, which were the vertical hinge rotated by 90° and 45°, respectively. Furthermore, as we showed in Fig. 3, symmetry detection is tuned to the angle of yaw of the vertical hinge surface: maximum facilitation occurs at about 45° of yaw. Increasing the yaw further reduces facilitation. This reduction of facilitation cannot be explained by a difficulty in seeing texture on a very slanted surface, as symmetry detection in the yaw condition at the same yaw is still similar to that in the frontoparallel condition. Thus, this tuning property may reflect 3D information selectivity in the symmetry detection mechanism.

3.1. Relation with 3D Computation

Computationally, to determine whether an image on the frontoparallel plane is symmetric, the visual system has to find correspondence between local features across a symmetric axis. Such computation can be achieved either by applying an idiosyncratic filter (“symmetry detector”) to the image (Dakin & Hess, 1997; Dakin & Watt, 1994; Gurnsey et al., 1998; Osorio, 1996; Rainville & Kingdom, 1999, 2000, 2002; Scognamillo et al., 2003) or calculating the correlation between an image and its flipped version (“reverse mapping”) (Barlow & Reeves, 1979; Chen & Tyler, 2010; Csatho et al., 2004; Tjan & Liu, 2005; van der Helm & Leeuwenberg, 1996; Wagemans, 1993). In our experiment, in addition to the correspondence computation for symmetry, there was also a correspondence computation for depth. Thus, it is reasonable to ask how the 3D computation affects symmetry detection.

In our experiment, the 3D information was carried by the disparity between the left and the right eye images. Hence, visual performance was also affected by finding a correspondence between the left and right eye images. To resolve the binocular correspondence problem, it is suggested that, in the visual system, units tuned to different disparities but the same locations would inhibit each other while the units tuned to the same disparities but different locations would facilitate each other (Marr, 1982; Marr & Poggio, 1976).

The interaction between the symmetry and depth computations might explain some aspects of our data. In the frontoparallel condition, dots in the same symmetry pair were also at the same depth. Hence, the association between the two dots in a symmetric pair may be enhanced by an iso-depth facilitation from the depth computation. On the other hand, in the step, random checkerboard and vertical shear conditions, the two dots in a symmetry pair were not at the same depth and thus the symmetry computation would not benefit from iso-depth facilitation. As a result, the thresholds for these conditions were higher than that for the frontoparallel condition. However, this cannot explain the result in the yaw condition which had the same threshold as the frontoparallel condition even though the two dots in a symmetry pair were not at the same depth.

In disparity gradient (Pollard, Mayhew, & Frisby, 1985; Tyler, 1973), units tuned to different locations and disparities can still facilitate each other as long the ratio of depth to distance is less than 1. This algorithm may account for our yaw condition result. In this condition, while the two points in a symmetry pair were at different depths, the disparity gradient between them was less than 1 as long as the slant angle was less than 45°. The yaw condition might retain much of the iso-depth facilitation which was available in the frontoparallel condition. As a result, both conditions had a similar threshold. However, this facilitation occurs only when the disparity gradient is less than 1 (Pollard et al., 1985), corresponding to the slant angle being less than 45°. In our result, the threshold for the yaw condition at 60° slant, which had a disparity gradient close to 2, was about the same as for the frontoparallel condition. This is inconsistent with what one would expect from disparity gradient computation. Furthermore, the disparity gradient cannot explain the threshold reduction in the vertical hinge condition. In order to explain the difference between the vertical hinge and the frontoparallel or pitch, one would require a mechanism that provides a greater facilitation to symmetry detection in the hinge than in the pitch condition. However, an image in the vertical hinge condition contained as many pairs at a given depth as an image in the pitch condition. The only difference between the two conditions was that the dot pairs at different depths were arranged in different ways. Thus, any depth computation based on a comparison between local features cannot provide the extra facilitation needed to explain our result. Instead, our result suggests that it is necessary for the symmetry detection mechanism to access the global 3D configuration in a scene.

It is reported that symmetry can help a human observer to determine the orientation of a 3D surface (Saunders & Knill, 2001) and to discriminate between 3D objects (Chan, Stevenson, Li, & Pizlo, 2006; Li & Pizlo, 2011). These results suggest that 2D symmetry processing occurs before or no later than 3D object processing. On the other hand, our result, which shows that 2D symmetry detection is affected by 3D configurations, suggests that, instead, it is 3D configuration processing which occurs before, or no later than, 2D symmetry processing. Put together, it seems that the visual processing of 2D symmetry and 3D configuration comes

together. This may be achieved by a template specialized for 3D symmetric objects, or by a reciprocal information exchange between a 3D object mechanism and 2D symmetry detector. The former is consistent with a theory suggesting that it is possible to reconstruct a 3D object from a single 2D image by assuming the object is symmetric (Li et al., 2011; Pizlo, 2008; Saunders & Knill, 2001). The empirical evidence for this theory is mainly from studies on skewed symmetry, which is an orthographic projection of a symmetry pattern on a slanted plane (Wagemans, van Gool, Swinnen, & van Horebeek, 1993). A human observer can easily detect skewed symmetry (Sawada & Pizlo, 2008) and use it to perceive 3D surfaces (Saunders & Knill, 2001) or objects (Chan et al., 2006; Li et al., 2011; Pizlo, Li et al., 2014; Sawada, 2010). This is possible because a human observer always perceives skewed symmetry as bilateral symmetry in depth (Wagemans, 1992, 1993). If this is the case, then, our result would indicate that such a 3D template would include not only symmetry on a slanted plane, as suggested by the studies of skewed symmetry, but also symmetry on two sides of a corner, as suggested by our hinge conditions.

4. Conclusion

To conclude, symmetry detection is subject to the 3D configuration of a scene. Symmetry detection deteriorates when the corresponding image elements across the symmetry axis are not coplanar, and improves when the 3D dihedral edge in the stimulus matches the 2D symmetry axis. Thus, symmetry detection in the human vision system is not solely based on an analysis of projected 2D images on the retina. Instead, it is based on an analysis of 3D structures in the scene.

Acknowledgment

Supported by NSC 99-2410-H-002-081-MY3 and NSC 102-2420-H-002-018-MY3 to C.C.C.

References

Barlow, H. B., & Reeves, B. C. (1979). The versatility and absolute efficiency of detecting mirror symmetry in random dot displays. *Vision Research, 19*(7), 783–793.

Bertone, A., & Faubert, J. (2002). The interactive effects of symmetry and binocular disparity on visual surface representation [Abstract]. *Journal of Vision, 2*, 94a.

Brainard, D. H. (1997). The psychophysics toolbox. *Spatial Vision, 10*(4), 433–436.

Carmody, D. P., Nodine, C. F., & Locher, P. J. (1977). Global detection of symmetry. *Perceptual and Motor Skills, 45*, 1267–1273.

Chan, M. W., Stevenson, A. K., Li, Y., & Pizlo, Z. (2006). Binocular shape constancy from novel views: The role of a priori constraints. *Perception and Psychophysics, 68*(7), 1124–1139.

Chen, C. C., & Tyler, C. W. (2008). Excitatory and inhibitory interaction fields of flankers revealed by contrast-masking functions. *Journal of Vision, 8*(4), 10.1–10.14. http://dx.doi.org/10.1167/8.4.10.

Chen, C. C., & Tyler, C. W. (2001). Lateral sensitivity modulation explains the flanker effect in contrast discrimination. *Proceedings Biological Sciences, 268*(1466), 509–516.

Chen, C. C., & Tyler, C. W. (2002). Lateral modulation of contrast discrimination: Flanker orientation effects. *Journal of Vision, 2*(6), 520–530. http://dx.doi.org/10.1167/2.6.8.

Chen, C. C., & Tyler, C. W. (2010). Symmetry: Modeling the effects of masking noise, axial cueing and salience. *PLoS ONE, 5*(4), e9840.

Corballis, M. C., & Roldan, C. E. (1975). Detection of symmetry as a function of angular orientation. *Journal of Experimental Psychology Human Perception and Performance, 104*, 221–230.

Csatho, A., van der Vloed, G., & van der Helm, P. A. (2004). The force of symmetry revisited: Symmetry-to-noise ratios regulate (a)symmetry effects. *Acta Psychologica, 117*(3), 233–250.

Dakin, S. C., & Hess, R. F. (1997). The spatial mechanisms mediating symmetry perception. *Vision Research, 37*(20), 2915–2930.

Dakin, S. C., & Watt, R. J. (1994). Detection of bilateral symmetry using spatial filters. *Spatial Vision, 8*(4), 393–413.

De Kuijer, J., Deregowski, J. B., & McGeorge, P. (2004). The influence of visual symmetry on the encoding of objects. *Acta Psychologica, 116*, 75–91.

Gurnsey, R., Herbert, A. M., & Kenemy, J. (1998). Bilateral symmetry embedded in noise is detected accurately only at fixation. *Vision Research, 38*(23), 3795–3803.

Huang, P. C., Chen, C. C., & Tyler, C. W. (2012). Collinear facilitation over space and depth. *Journal of Vision, 12*(2), 1–9, pii: 20.

Huang, P. C., Hess, R. F., & Dakin, S. C. (2006). Flank facilitation and contour integration: Different sites. *Vision Research, 46*(21), 3699–3706.

Kanade, T. (1981). Recovery of the three-dimensional shape of an object from a single view. *Artificial Intelligence, 17*, 409–460.

Koffka, K. (1935). *Principles of gestalt psychology*. New York: Harcourt, Brace, & World.

Kontsevich, L. L., & Tyler, C. W. (1999). Bayesian adaptive estimation of psychometric slope and threshold. *Vision Research, 39*, 2729–2737.

Li, Y., Sawada, T., Shi, Y., Kwon, T., & Pizlo, Z. (2011). A Bayesian model of binocular perception of 3D mirror symmetrical polyhedra. *Journal of Vision, 11*(4). http://dx.doi.org/10.1167/11.4.11, pii: 11.

Li, Y., & Pizlo, Z. (2011). Depth cues versus the simplicity principle in 3D shape perception. *Topics in Cognitive Science, 3*(4), 667–685.

Liu, Z., & Kersten, D. (2003). Three-dimensional symmetric shapes are discriminated more efficiently than asymmetric ones. *Journal of the Optical Society of America A, 20*(7), 1331–1340.

Locher, P., & Smets, G. (1992). The influence of stimulus dimensionality and viewing orientation on detection of symmetry in dot patterns. *Bulletin of the Psychonomic Society, 30*, 43–46.

Marr, D. (1982). *Vision*. San Francisco: W.H. Freeman.

Marr, D., & Poggio, T. (1976). Cooperative computation of stereo disparity. *Science, 194*, 283–287.

Masson, M. E. (2011). A tutorial on a practical Bayesian alternative to null-hypothesis significance testing. *Behavior Research, 43*, 679–690.

Osorio, D. (1996). Symmetry detection by categorization of spatial phase, a model. *Proceedings of the Royal Society of London B, 263*, 105–110.

Pizlo, Z. (2008). *3D shape: Its unique place in visual perception*. Cambridge, MA: MIT Press.

Pizlo, Z., Li, Y., Sawada, T., & Steinman, R. M. (2014). *Making a machine that sees like us*. Oxford: Oxford University Press.

Pizlo, Z., Sawada, T., Li, Y., Kropatsch, W. G., & Steinman, R. M. (2010). New approach to the perception of 3D shape based on veridicality, complexity, symmetry and volume. *Vision Research, 50*(1), 1–11.

Poirier, F. J. A. M., & Wilson, H. R. (2010). A biologically plausible model of human shape symmetry perception. *Journal of Vision, 10*, 1–16.

Polat, U., & Sagi, D. (1993). Lateral interactions between spatial channels: Suppression and facilitation revealed by lateral masking experiments. *Vision Research, 33*(7), 993–999.

Polat, U., & Sagi, D. (1994). The architecture of perceptual spatial interactions. *Vision Research, 34*(1), 73–78.

Pollard, S. B., Mayhew, J. E., & Frisby, J. P. (1985). PMF: A stereo correspondence algorithm using a disparity gradient limit. *Perception, 4*, 449–470.

Qiu, C., Kersten, D., & Olman, C. A. (2013). Segmentation decreases the magnitude of the tilt illusion. *Journal of Vision, 13*(13), 19. http://dx.doi.org/10.1167/13.13.19.

Rainville, S. J., & Kingdom, F. A. (1999). Spatial-scale contribution to the detection of mirror symmetry in fractal noise. *Journal of Optical Society of America Image Society Vision, 16*(9), 2112–2123.

Rainville, S. J., & Kingdom, F. A. (2000). The functional role of oriented spatial filters in the perception of mirror symmetry-psychophysics and modeling. *Vision Research, 40*(19), 2621–2644.

Rainville, S. J., & Kingdom, F. A. (2002). Scale invariance is driven by stimulus density. *Vision Research, 42*, 351–367.

Rouder, J. N., Speckman, P. L., Sun, D., & Iverson, G. (2009). Bayesian *t* tests for accepting and rejecting the null hypothesis. *Psychonomic Bulletin and Review, 16*(2), 225–237.

Saunders, J. A., & Knill, D. C. (2001). Perception of 3D surface orientation from skew symmetry. *Vision Research, 41*, 3163–3183.

Sawada, T. (2010). Visual detection of symmetry of 3D shapes. *Journal of Vision, 10*(6), 4. http://dx.doi.org/10.1167/10.6.4.

Sawada, T., & Pizlo, Z. (2008). Detection of skewed symmetry. *Journal of Vision, 8*(5), 14.1–14.18. http://dx.doi.org/10.1167/8.5.14.

Scognamillo, R., Rhodes, G., Morrone, C., & Burr, D. (2003). A feature-based model of symmetry detection. *Proceedings Biological Sciences, 270*(1525), 1727–1733.

Tjan, B. S., & Liu, Z. (2005). Symmetry impedes symmetry discrimination. *Journal of Vision, 5*(10), 888–900.

Tyler, C. W. (1973). Stereoscopic vision: Cortical limitations and a disparity scaling effect. *Science, 181*, 276–278.

Tyler, C. W. (1994). Theoretical issues in symmetry perception. *Spatial Vision, 8*(4), 383–391.

Tyler, C. W., Hardage, L., & Miller, R. T. (1995). Multiple mechanisms for the detection of mirror symmetry. *Spatial Vision, 9*, 79–100.

Tyler, C. W., & Kontsevich, L. L. (1995). Mechanisms of stereoscopic processing: Stereoattention and surface perception in depth reconstruction. *Perception, 24*, 127–153.

Utall, W. R. (1983). *Visual form detection in three-dimensional space*. Hillsdale, NJ: Erlbaum.

van der Helm, P. A., & Leeuwenberg, E. L. (1996). 'Goodness of visual regularities: A nontransformational approach. *Psychological Research Psychologische Forschung, 103*(3), 429–456.

van der Vloed, G., Csathó, Á., & van der Helm, P. A. (2005). Symmetry and repetition in perspective. *Acta Psychologica, 120*, 74–92.

Vetter, T., & Poggio, T. (1994). Symmetric 3D objects are an easy case for 2D object recognition. *Spatial Vision, 8*(4), 443–453.

Wagemans, J. (1992). Perceptual use of nonaccidental properties. *Canadian Journal of Psychology, 46*(2), 236–279.
Wagemans, J. (1993). Skewed symmetry: A nonaccidental property used to perceive visual forms. *Journal of Experimental Psychololgy Human Perception and Performance, 19*(2), 364–380.
Wagemans, J. (1995). Detection of visual symmetries. *Spatial Vision, 9*, 9–32.
Wagemans, J., van Gool, L., Swinnen, V., & van Horebeek, J. (1993). Higher-order structure in regularity detection. *Vision Research, 33*, 1067–1088.
Wagenmaker, E. J. (2007). A practical solution to the pervasive problems of *p* values. *Psychonomic Bulletin and Review, 14*(5), 779–804.
Wu, C. C., & Chen, C. C. (2014). The symmetry detection mechanisms are color selective. *Scientific Reports, 4*, 3893.